Mapping the dominant regions of the phase space associated with $c\bar{c}$ production relevant for the prompt atmospheric neutrino flux

Victor P. Goncalves[*]
Instituto de Física e Matemática, Universidade Federal de Pelotas (UFPel), Caixa Postal 354, CEP 96010-900 Pelotas, RS, Brazil

Rafał Maciuła[†]
Institute of Nuclear Physics PAN, PL-31-342 Cracow, Poland

Roman Pasechnik[‡]
Department of Astronomy and Theoretical Physics, Lund University, 22362 Lund, Sweden

Antoni Szczurek[§]
University of Rzeszów, PL-35-959 Rzeszów, Poland and Institute of Nuclear Physics PAN, PL-31-342 Cracow, Poland

(Received 23 August 2017; published 28 November 2017)

We present a detailed mapping of the dominant kinematical domains contributing to the prompt atmospheric neutrino flux at high neutrino energies by studying their sensitivity to the cuts on several kinematical variables crucial for charm production in cosmic ray scattering in the atmosphere. This includes the maximal center-of-mass energy for proton-proton scattering, the longitudinal momentum fractions of partons in the projectile (cosmic ray) and target (nucleus of the atmosphere), the Feynman x_F variable, and the transverse momentum of charm quark/antiquark. We find that the production of neutrinos with energies larger than $E_\nu > 10^7$ GeV is particularly sensitive to the c.m. energies larger than the ones at the LHC and to the longitudinal momentum fractions in the projectile $10^{-8} < x < 10^{-5}$. Clearly, these are regions where we do not control the parton, in particular, gluon, densities. We also analyze the characteristic theoretical uncertainties in the charm production cross section coming from its QCD modeling. The precision data on the prompt atmospheric neutrino flux can efficiently constrain the mechanism of heavy quark production and underlying QCD dynamics in kinematical ranges beyond the reach of the current collider measurements.

DOI: 10.1103/PhysRevD.96.094026

I. INTRODUCTION

The recent detection of ultrahigh-energy neutrino events with deposited energies up to a few PeV by the IceCube Observatory sets the beginning of neutrino astronomy [1–3] (for a review of IceCube potential for neutrino astronomy, see, e.g., Ref. [4]). It is mandatory to know the flux of atmospheric neutrino produced in cosmic ray interactions with nuclei in Earth's atmosphere at different energies with high precision as an unavoidable background for cosmic neutrino studies. In recent years, the atmospheric high-energy neutrino flux became accessible to the experimental studies and, in particular, was constrained by several neutrino observatories [5–8].

The available data indicate that the neutrino flux observed in the experiment is dominated at low energies ($E_\nu \lesssim 10^5$ GeV) by atmospheric neutrinos that arise from the decay of light mesons (pions and kaons), denoted as the "conventional" atmospheric neutrino flux [9–11], whereas the data for the higher energies ($E_\nu \gtrsim 10^7$ GeV) are most probably associated with cosmic neutrinos. In the intermediate energy range ($10^5 < E_\nu < 10^7$ GeV), it is expected that the prompt atmospheric neutrino flux associated with the decay of heavy flavored hadrons, composed of heavy quarks, becomes important [12–14]. In particular, it is typically considered that this contribution dominates the atmospheric neutrino flux for large neutrino energies ($E_\nu > 10^6$ GeV).

This expectation can be easily understood. The increasing competition between the interaction and decay lengths for pions and kaons at high energies implies a reduction of the neutrino flux associated with the decay of these particles. This behavior is related to the fact that the long-lived high-energy light mesons interact and lose their energy before decaying into neutrinos. In contrast, in the case of heavy hadrons, they have short lifetimes and decay into neutrinos almost immediately after their production. Consequently, at

[*]barros@ufpel.edu.br
[†]Rafal.Maciula@ifj.edu.pl
[‡]Roman.Pasechnik@thep.lu.se
[§]Antoni.Szczurek@ifj.edu.pl

very high energies, the atmospheric neutrino flux is expected to arise from semi-leptonic decays of heavy, in particular, charmed, hadrons.

Thus, the precise knowledge of the prompt atmospheric flux is crucial for the determination of the cosmic neutrino flux. This subject has been a theme of intense debate in the literature, mainly because the calculation requires good knowledge of the heavy quark production cross section at high energies. In the last two years, results of many calculations of this flux were presented [14–22], focusing on the determination of the theoretical uncertainties present in the QCD calculations. These uncertainties are typically associated, for example, with the choice of the heavy quark masses and factorization and renormalization scales, as well as the contribution of higher-order corrections, the choice of the parton distribution functions (PDFs) and the treatment of QCD dynamics at high energies (very small x). The overall theoretical uncertainty in QCD predictions of the prompt neutrino flux has been estimated to be a factor of 3 or a bit larger in Ref. [13]. The impact of nuclear effects, saturation, and low-x resummation was studied in detail in Ref. [17]. The recent LHC data for the prompt heavy quark production cross sections (see, e.g., Refs. [23,24]) significantly reduced some of these uncertainties, with direct impact on the predictions for the prompt neutrino flux; however, several questions still remain open.

The prompt neutrino flux is usually calculated using the semianalytical Z-moment approach, proposed many years ago in Ref. [12] and discussed in detail, e.g., in Refs. [16,25]. One of the main inputs in this approach is the Feynman x_F distribution for the heavy quark production in hadronic collisions. As discussed, e.g., in Refs. [25,26], it is expected that the main contribution to the prompt neutrino flux comes from large values of x_F that are associated with the heavy quark production at forward rapidities. Moreover, the production of neutrinos at a given neutrino energy E_ν is determined by collisions of cosmic rays with nuclei in the atmosphere at energies that are a factor of order 100–1000 larger. One also has that the prompt neutrino flux measured in the kinematical range that is probed by the IceCube Observatory and future neutrino telescopes is directly associated with the treatment of the heavy quark cross section at high energies. Currently, different experiments at the LHC probe a limited range in rapidity. In particular, they do not cover rapidities larger than 4.5, which corresponds to relatively small values of $x_F \lesssim 0.1$. Therefore, the D meson production in the kinematical range of large x_F values is not covered by the LHC detectors.

The main motivation of the current study is to clarify the kinematical range of energies and rapidities in the heavy quark production that determine the prompt atmospheric neutrino flux in the range probed by the IceCube Observatory. Such an aspect is fundamental if we would like to reduce the current theoretical uncertainties. Moreover, as the IceCube 2 program [27] is expected to measure neutrinos with energies that are 3 orders of magnitudes larger than the current coverage, it also will help to define what the theoretical issues are that should be resolved in order to obtain realistic predictions for the future neutrino telescopes.

In this paper, we concentrate on $c\bar{c}$ production to understand to which extent the calculated prompt neutrino flux is reliable. We therefore neglect the $b\bar{b}$ production, as well as nuclear effects. The $b\bar{b}$ component gives about 10% contribution to the corresponding x_F distribution and thus to the neutrino flux [17].

The paper is organized as follows. In the next section, we present a brief review of the Z-moment formalism for the calculation of the prompt atmospheric neutrino flux. Moreover, we describe the main assumptions of our analysis and present a comparison of our results and those obtained by the Prosa Collaboration [21]. In Sec. III, we discuss the different cuts assumed in the calculations and analyze their impact on the neutrino flux, focusing on $E_\nu > 10^6$ GeV. Finally, in Sec. IV, we summarize our main conclusions.

II. PROMPT ATMOSPHERIC NEUTRINO FLUX

In order to determine the prompt atmospheric neutrino flux at the detector level we should describe the production and decay of the heavy hadrons as well as the propagation of the associated particles through the atmosphere. The evolution of the inclusive particle fluxes in the Earth's atmosphere can be obtained using the Z-moment approach [12]. In this approach, a set of coupled cascade equations for the nucleons, heavy mesons, and leptons (and their antiparticles) fluxes is solved, with the equations being expressed in terms of the nucleon-to-hadron (Z_{NH}), nucleon-to-nucleon (Z_{NN}), hadron-to-hadron (Z_{HH}), and hadron-to-neutrino ($Z_{H\nu}$) Z moments. For a detailed discussion of the cascade equations, see, e.g., Refs. [12,16]. These moments are inputs in the calculation of the prompt neutrino flux associated with production of a heavy hadron H and its decay into a neutrino ν in the low- and high-energy regimes, which are given, respectively, by [12]

$$\phi_\nu^{H,\mathrm{low}} = \frac{Z_{NH}(E) Z_{H\nu}(E)}{1 - Z_{NN}(E)} \phi_N(E, 0), \tag{1}$$

$$\phi_\nu^{H,\mathrm{high}} = \frac{Z_{NH}(E) Z_{H\nu}(E)}{1 - Z_{NN}(E)} \frac{\ln(\Lambda_H/\Lambda_N)}{1 - \Lambda_N/\Lambda_H} \frac{m_H c h_0}{E \tau_H} f(\theta) \phi_N(E, 0), \tag{2}$$

where $H = D^0$, D^+, D_s^+, Λ_c for charmed hadrons, $\phi_N(E, 0)$ is a primary flux of nucleons in the atmosphere, m_H is the decaying particle's mass, τ_H is the proper lifetime of the hadron, $h_0 = 6.4$ km, $f(\theta) \approx 1/\cos\theta$ for $\theta < 60°$, and the effective interaction lengths Λ_i are given by $\Lambda_i = \lambda_i/(1 - Z_{ii})$, with λ_i being the associated interaction length ($i = N, H$). The expected prompt neutrino flux in the detector can be estimated using the geometric interpolation formula

$$\phi_\nu = \sum_H \frac{\phi_\nu^{H,\mathrm{low}} \cdot \phi_\nu^{H,\mathrm{high}}}{\phi_\nu^{H,\mathrm{low}} + \phi_\nu^{H,\mathrm{high}}}. \quad (3)$$

In what follows, we will focus on vertical fluxes ($\theta = 0$) and assume that the cosmic ray flux ϕ_N can be described by a broken power-law spectrum [26], with the incident flux being represented by protons ($N = p$). Moreover, we will assume that the charmed hadron Z moments can be expressed in terms of the charm Z moment as follows: $Z_{pH} = f_H \times Z_{pc}$, where f_H is the fraction of charmed particle that emerges as a hadron H. As in Ref. [25], we will assume that $f_{D^0} = 0.565$, $f_{D^+} = 0.246$, $f_{D_s^+} = 0.080$, and $f_{\Lambda_c} = 0.094$.

It is important to emphasize that the composition of the particle content of the ultrahigh-energy cosmic rays in the region beyond the ankle ($E \approx 5 \times 10^9$ GeV) is still an open question and no clear consensus exists. As the computation of the prompt atmospheric neutrino flux requires a folding of the heavy quark cross section with the incoming cosmic flux, both aspects increase the uncertainty in the predictions for the flux in the high-energy regime. This point has been recently discussed in detail in Refs. [17,21].

The charm Z moment at high energies can be expressed by

$$Z_{pc}(E) = \int_0^1 \frac{dx_F}{x_F} \frac{\phi_p(E/x_F)}{\phi_p(E)} \frac{1}{\sigma_{pA}(E)} \frac{d\sigma_{pA\to\mathrm{charm}}(E/x_F)}{dx_F}, \quad (4)$$

where E is the energy of the produced particle (charm), x_F is the Feynman variable, σ_{pA} is the inelastic proton-air cross section, which we assume to be given as in Ref. [14], and $d\sigma/dx_F$ is the differential cross section for the charm production, which we assume to be given by $d\sigma_{pA\to\mathrm{charm}}/dx_F = 2d\sigma_{pA\to c\bar{c}}/dx_F$.

We compute the prompt neutrino flux associated with charmed hadrons by evaluating all quantities entering the different terms of Eq. (3). In our analysis, we closely follow Refs. [17,26]. In the analysis of Eq. (4), we will use the standard QCD collinear factorization formalism, allowing us to calculate the charm production cross section [28]. In the leading-order collinear factorization approach, the differential cross section can be written as

$$\frac{d\sigma}{dy_1 dy_2 d^2p_T} = \frac{1}{16\pi^2 \hat{s}} \times \Big[\overline{|\mathcal{M}_{gg\to c\bar{c}}|^2} x_1 g(x_1,\mu_f^2) x_2 g(x_2,\mu_f^2) + \sum_f \overline{|\mathcal{M}_{q\bar{q}\to c\bar{c}}|^2} x_1 q_f(x_1,\mu_f^2) x_2 \bar{q}_f(x_2,\mu_f^2) + \sum_f \overline{|\mathcal{M}_{q\bar{q}\to c\bar{c}}|^2} x_1 \bar{q}_f(x_1,\mu_f^2) x_2 q_f(x_2,\mu_f^2) \Big], \quad (5)$$

where p_T is the heavy quark transverse momentum, and y_1 and y_2 are the charm and anticharm rapidities, respectively. The distribution in x_F is obtained by an appropriate binning. The PDFs will be assumed to be given by the CT14 parametrization [29] and the hard scattering will be estimated at the leading order taking into account both $gg \to c\bar{c}$ and $q\bar{q} \to c\bar{c}$ subprocesses. The contribution of the next-to-leading-order corrections for the x_F distribution will be taken into account by multiplying our predictions by an effective K factor that depends on x_F, as proposed in Ref. [26], which is given by $K(E,x_F) = 1.36 + 0.42\ln[\ln(E/\mathrm{GeV})] + [3.40 + 18.7(E/\mathrm{GeV})]^{-0.43} - 0.079\ln(E/\mathrm{GeV}) \cdot x_F^{1.5}$. We assume $m_c = 1.5$ GeV, the factorization and renormalization scales are taken as $\mu_f^2 = \mu_r^2 = m_T^2 \equiv (p_T^2 + m_c^2)$. From previous studies of the charm production [14,15], we expect that the predictions for the D meson cross sections are sensitive to the choice of these scales. In particular, the magnitude of the cross section can be modified by the change of these scales, which has implications on the charm Z moment. However, we do not expect a strong modification of the x_F dependence of the charm cross sections. As a consequence, the conclusions associated with the impact of different kinematical cuts to be analyzed in the next section are not expected to be sensitive to the choice of μ_f and μ_r.

In the present analysis, we will disregard the nuclear effects, in particular, shadowing, i.e., we calculate the cross section for collisions on nuclei as $\sigma_{pA\to c\bar{c}} = Z \times \sigma_{pp\to c\bar{c}} + N \times \sigma_{pn\to c\bar{c}} \approx A \times \sigma_{pp\to c\bar{c}}$, where Z, N, and A are the number of protons, neutrons, and nucleons in the nucleus of the target, respectively. In practical calculations, we take ^{14}N nucleus as the most representative one. A more refined analysis is possible, but would shadow our discussion of the selected issues.

Moreover, we will calculate the effective hadronic interaction lengths Λ_i and the Z_{pp}, Z_{HH}, and $Z_{H\nu}$ moments as performed in Ref. [15]. Although we have done several approximations to compute the prompt neutrino flux, our

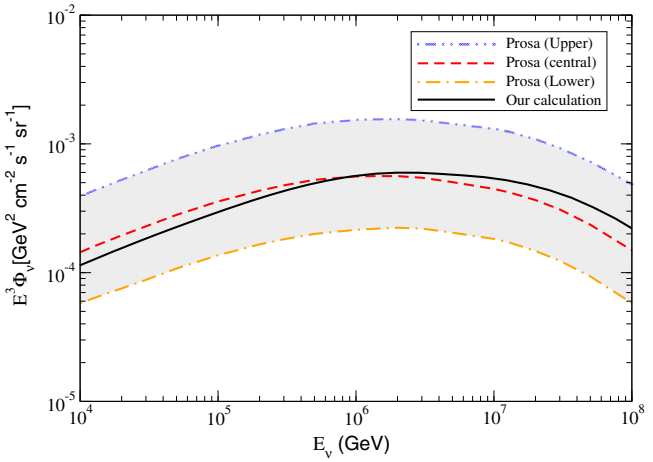

FIG. 1. Comparison of our predictions for the prompt neutrino flux and the Prosa results [21].

result is similar to the central prediction of the Prosa Collaboration [21], as shown in Fig. 1. In this figure, we also show the current theoretical uncertainty band present in one of the most sophisticated calculations of the neutrino flux. Although the available data from collider experiments are used in Ref. [21] as an input to constrain the main uncertainties present in the treatment of heavy quark production, the associated predictions for the neutrino flux are still uncertain. The main sources of uncertainty here are associated with the modeling of the cosmic ray composition and renormalization/factorization scale variations.

III. RESULTS

In this section, we wish to understand what the range is of several kinematical variables relevant for the production of the high-energy neutrinos observed recently by IceCube or for higher energies than possible at present. To realize the goal, we map the range of several kinematical variables, such as c.m. energies, charm transverse momentum (p_T), parton momentum fractions in the projectile (x_1) and target (x_2), and the Feynman x (x_F). All of them determine the size of the cross section and, as a consequence, the energy dependence of the prompt neutrino flux.

Let us analyze first how the flux of neutrinos from semileptonic decays of D mesons depends on the maximal center-of-mass collision energy included in the calculation. In Fig. 2, we present our results obtained for different values of the maximal energies considered in the analysis of the differential cross section in Eq. (4). As x_F is integrated and $d\sigma/dx_F$ is probed at the energy E/x_F, we have that $Z_{pc}(E)$ may be influenced by the behavior of distribution at higher energies. In our calculation, we consider three different values for the maximum center-of-mass energy allowed in the pp collision that generates the heavy quark pair. For comparison, the full prediction for the flux, denoted as "no cuts" in the figure, is presented. Here, no energy limitations

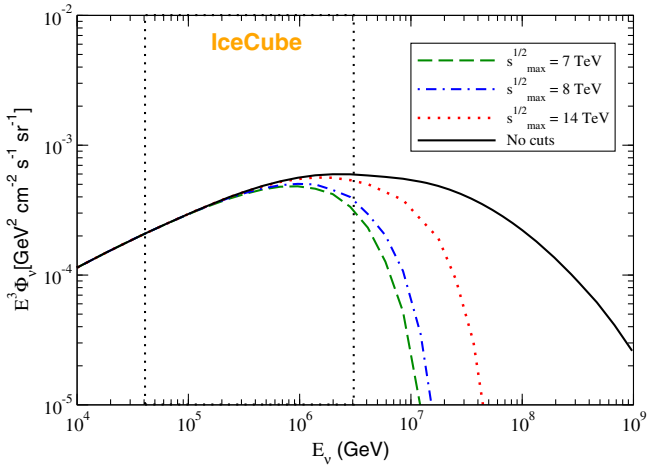

FIG. 2. Impact of different cuts on the maximal center-of-mass pp collision energy for the prompt neutrino flux.

were imposed. Moreover, for illustration, the energy range probed by the recent IceCube data [3] is shown as well. The figure demonstrates that the flux depends on the cross section for heavy quark production in the LHC energy range and at even larger energies. The latter unexplored region can also have a direct impact on the flux at high neutrino energies ($E_\nu \geq 10^6$ GeV).

Moreover, our results indicate that the prompt neutrino flux for $E_\nu \gtrsim 10^7$ GeV is determined by the behavior of the differential cross section in the energy range beyond that probed in the Run 2 of the LHC. Consequently, the detection of prompt atmospheric neutrinos in this range by the IceCube experiment, its upgrade or by other future neutrino telescope, can significantly contribute to our understanding of several aspects associated with the heavy quark production at high energies. Whether we control at present the cross section for energies above those for the LHC is an open question, at least, in our opinion.

In Fig. 3, we present the sensitivity of the charm production cross section $d\sigma/dx_F$ (left panel) and the corresponding energy dependence of the prompt neutrino flux on x_1 cuts. The notation of the different curves indicate the range of x_1 values that is included in our calculations. The x_1 cut has a direct impact on the x_F distribution, strongly suppressing the distribution at large x_F. Regarding the neutrino flux presented in the right panel, we observe that the main contribution comes from the intermediate x_1 range ($0.2 < x_1 < 0.6$). These results demonstrate that the significant portion of the neutrino flux comes from very forward (large x_F) charm production, with the incident parton energy larger than 20% of the projectile nucleon energy at any probed neutrino energy.

Analogously, in Fig. 4, we show the corresponding sensitivity to the cuts on the target momentum fraction x_2. One finds that if the values of $x_2 \leq 10^{-5}$ are excluded, the x_F distribution gets strongly suppressed at intermediate and large x_F. In particular, our results indicate that the main contribution to the distribution at proton energy $E_p = 10^9$ GeV comes from the $10^{-7} < x < 10^{-5}$ range of gluon longitudinal momentum fractions.

Regarding the neutrino flux, one can see that, in the kinematical range probed by the recent IceCube data [3], one observes a strong sensitivity to the region of $x_2 < 10^{-5}$. For neutrino energies $E_\nu > 10^7$ GeV, even the region of $x_2 < 10^{-7}$ becomes important. These values of x are beyond those probed by the pp and ep colliders, currently and in the past. For instance, the charm production at the LHC (LHCb detector) is sensitive to $x_2 > 10^{-5}$, while the HERA data lead to constraints on the gluon distributions for $x_2 > 10^{-4}$. The smallest values of $x_2 \sim 10^{-6}$ can be obtained from the inclusive production of χ_c mesons [30,31] in pp collisions and in the exclusive J/Ψ photoproduction in hadronic collisions [32]. However, these possible constraints have not been used so far to extract the gluon distributions. The models of gluon distributions

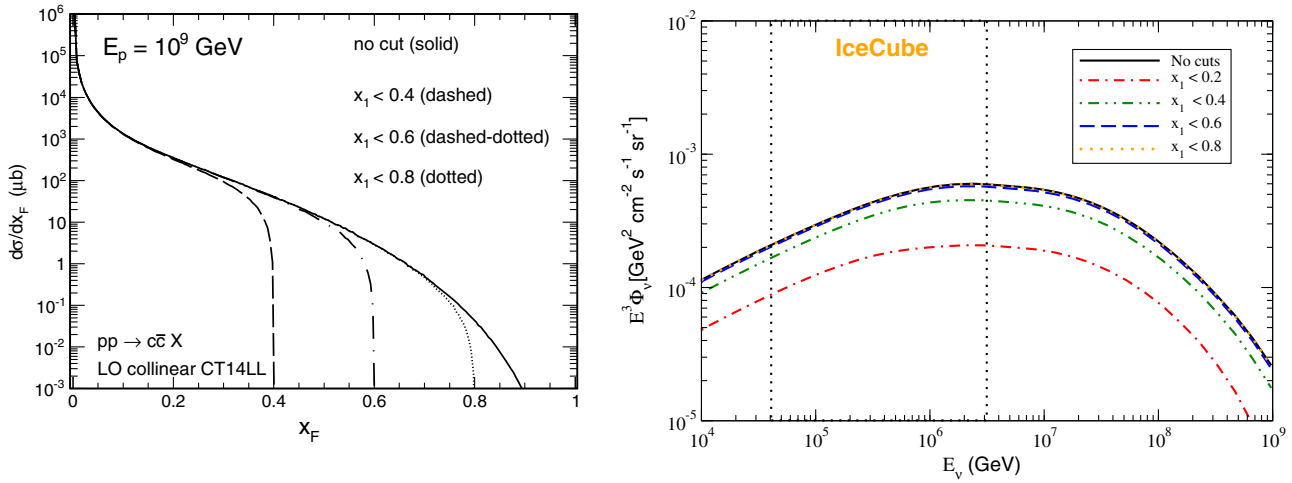

FIG. 3. Effect of x_1 cuts on the charm production cross section $d\sigma/dx_F$ (left) and prompt neutrino flux (right).

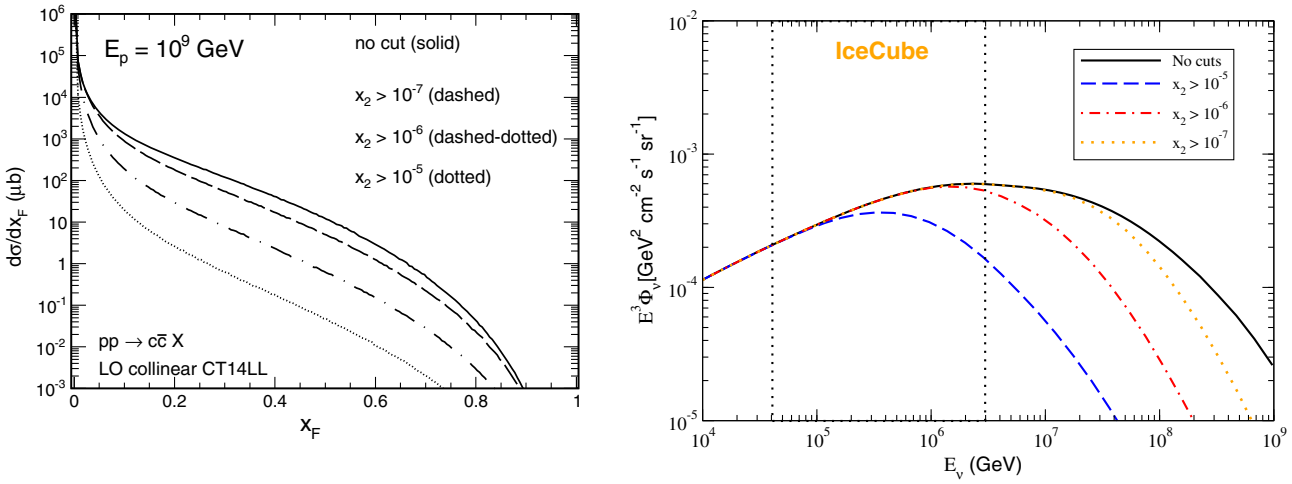

FIG. 4. Effect of x_2 cuts on the charm production cross section $d\sigma/dx_F$ (left) and prompt neutrino flux (right).

in proton for $x_2 < 10^{-5}$ are therefore rather uncertain (see, e.g., Ref. [33]). Consequently, the future neutrino telescopes will probe the prompt neutrino flux in a weakly explored small-x range of the QCD dynamics.

Very recently, however, in Ref. [34], the combined set of the LHCb data on D meson production at $\sqrt{s} = 5$, 7, and 13 TeV has been shown to constrain the gluon PDF reasonably well down to $x \sim 10^{-6}$. Namely, the combined analysis has resulted in an order-of-magnitude reduction of uncertainties in the gluon PDF compared with such well-known parametrizations as the NNPDF3.0 [33] (for a more recent alternative analysis of the low-x gluon PDF driven by the charm LHCb data, see, e.g., Ref. [35]). Implications of such a reduction in the gluon PDF uncertainties for the prompt neutrino flux have been discussed in Ref. [36].

In Fig. 5 (left panel), we present the results for the prompt neutrino flux for different cuts on the Feynman x_F variable. We find that the dominant contribution to the neutrino flux comes typically from x_F in the region $0.2 < x_F < 0.5$, which is consistent with our previous results for the impact of the x_1 and x_2 cuts. In Fig. 5 (right panel), we show a two-dimensional plot in (x_1, $\log_{10}x_2$) for this x_F range. For simplicity, in this calculation, only the gluon-gluon fusion was taken into account, which is the dominant mechanism at large energies (see below). In particular, one can see that the dominant contribution comes from the region of $x_1 \in (0.2 - 0.6)$ and $x_2 \in (10^{-8} - 10^{-5})$. We wish to stress that, in both these regions of longitudinal momentum fractions, gluon distribution is poorly constrained (see, e.g., Ref. [29]). The behavior of the x_F distribution at intermediate x_F is directly associated with the charm production at large rapidities, beyond those probed currently by the LHC detectors.

For completeness, in Fig. 6, we analyze the effect of cuts on the quark transverse momentum p_T on the prompt neutrino flux. Our results indicate that the prompt neutrino flux is mainly determined by the charm production with

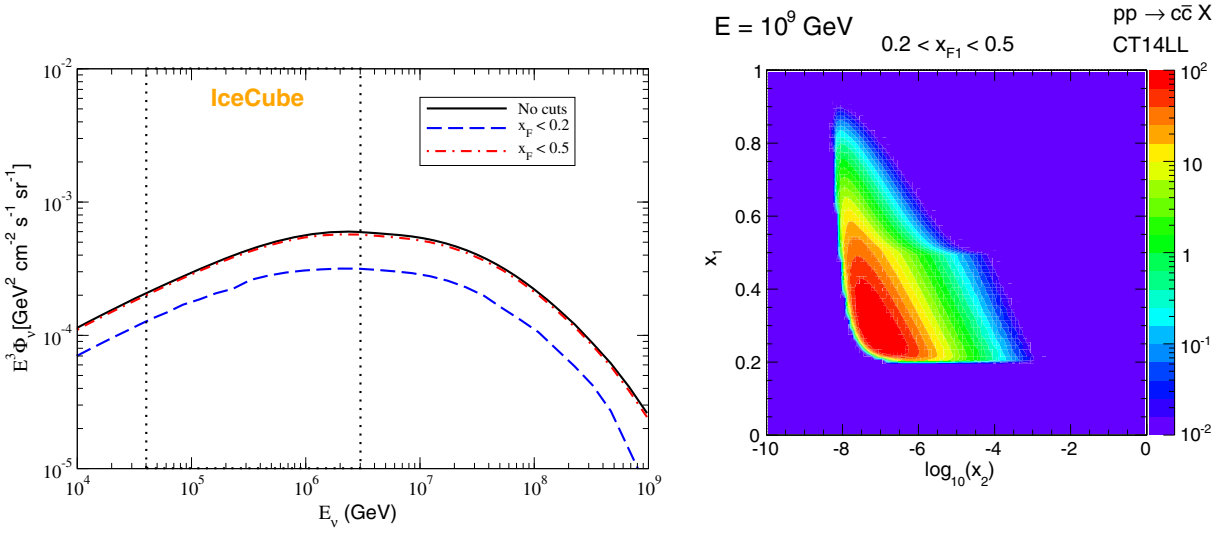

FIG. 5. Effect of cuts on the Feynman variable x_F on the prompt neutrino flux (left) and the two-dimensional differential cross section for charm production in pp collisions as a function of x_1 and $\log_{10}(x_2)$ (right).

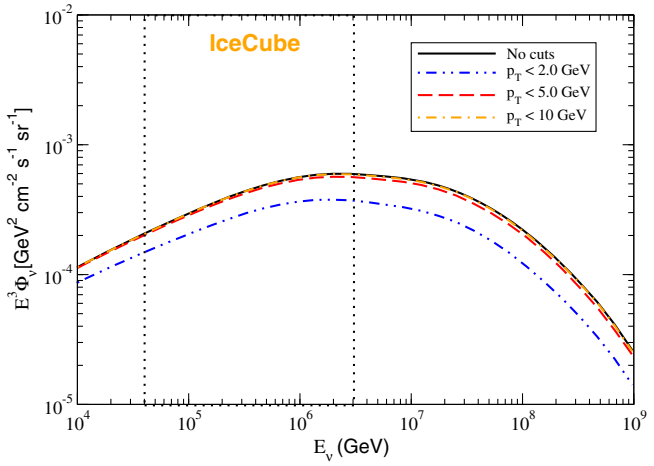

FIG. 6. Effect of cuts on the quark transverse momentum p_T on the prompt neutrino flux.

transverse momentum in the $0 < p_T < 2$ GeV range, but it also is sensitive to the $2 < p_T < 5$ GeV range. For instance, we have that, for $E_\nu = 10^8$ GeV, the small $-p_T$ range contributes with 56% to the neutrino flux, while the contribution of the $2 < p_T < 5$ GeV range is 36%. As the description of the transverse momentum spectra for the D meson production at the LHC in this p_T range has a larger theoretical uncertainty (see, e.g., Ref. [21]), it also implies a large uncertainty in the neutrino flux predictions in the kinematical range probed by the IceCube.

In order to estimate uncertainties of our conclusions caused by the model used to describe the primary nucleon flux, in Fig. 7, we compare the previous predictions obtained using the broken power low model with those derived assuming that the primary flux is described by the sharp knee (SK) one. This spectrum is based on a parametrization proposed in Ref. [37] given by

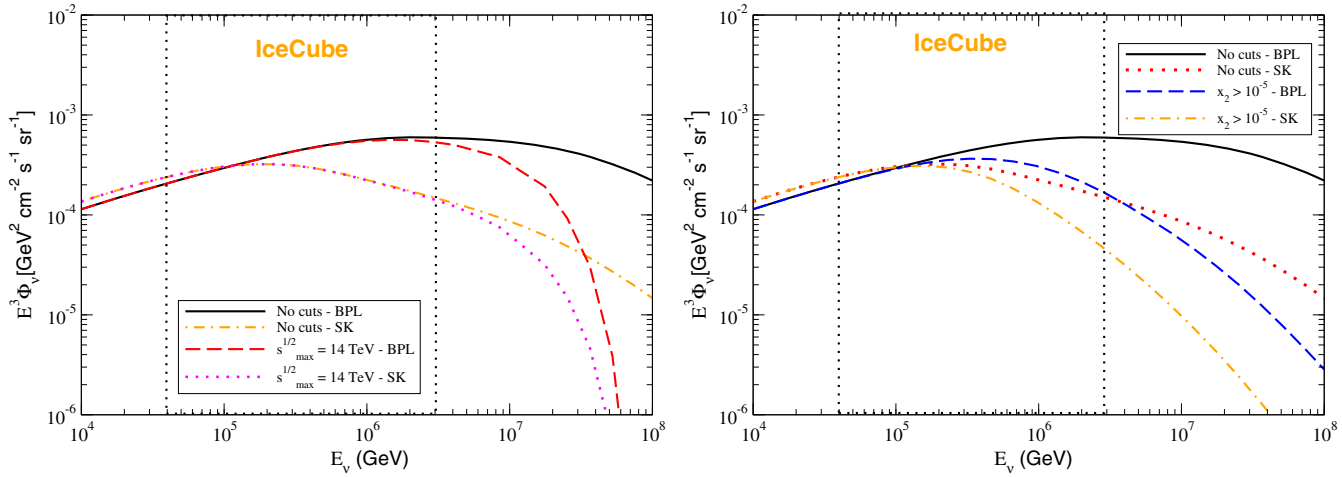

FIG. 7. Comparison between predictions for the neutrino flux obtained using the broken law power (BPL) and SK models for the primary nucleon flux considering cuts on the maximal center-of-mass pp collision energy (left) and the value of x_2 (right).

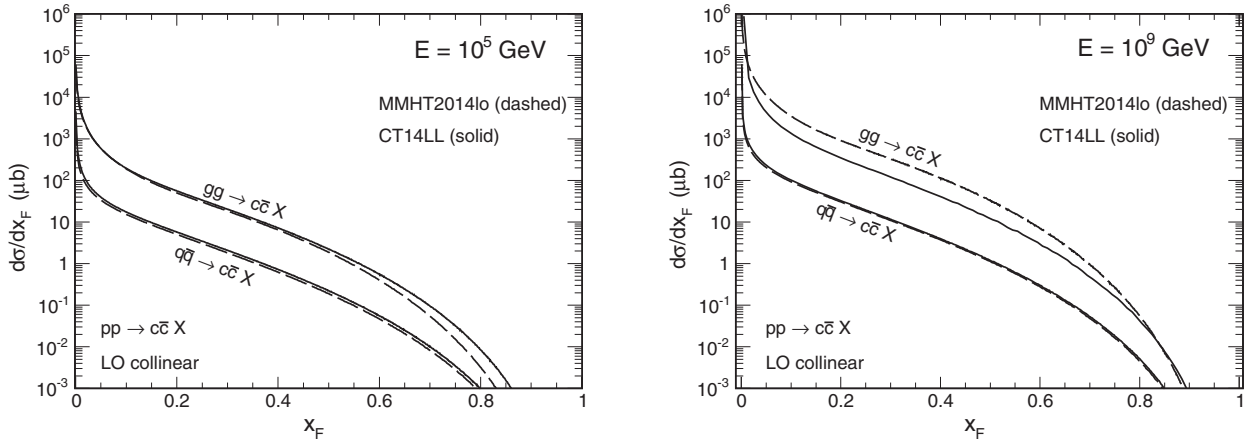

FIG. 8. Charm production cross section $d\sigma/dx_F$ obtained with the leading-order collinear factorization for two different energies (left and right) and for two different PDF sets. Here, the $gg \to c\bar{c}$ and $q\bar{q} \to c\bar{c}$ components are shown separately.

$$\phi_N(E,0) = I_0 E^{-\gamma_1 - 1}\left[1 + \left(\frac{E}{E_k}\right)^{\epsilon}\right]^{\frac{\gamma_1-\gamma_2}{\epsilon}}. \qquad (6)$$

Such spectrum starts at low energy ($E \ll E_k$) following approximately a power-law behavior: $I_0 E^{-\gamma_1-1}$. The spectral index changes from γ_1 to γ_2, creating a "knee" at $E = E_k$, with a sharpness parameter ϵ. We choose parameter values that fit the H3a spectrum, used in several recent studies [14,15,17], with a relative error of less than 10% in the range 100 GeV–10 PeV: $\gamma_1 = 1.65$, $\gamma_2 = 2.4$, $E_k = 1.2$ PeV, $\epsilon = 3.0$, and $I_0 = 11500$ $(\mathrm{Gev}^{1.65}\,\mathrm{s\,m^2\,sr})^{-1}$. The results presented in Fig. 7 indicate that the energy dependence of the neutrino flux is strongly sensitive on the model used to describe the primary neutrino flux, in agreement with the results obtained, e.g., in Ref. [14]. The impact of the maximum c.m. energy is analyzed in the left panel. We have that, for both primary flux models, the behavior of the neutrino flux at $E_\nu \gtrsim 2 \times 10^6$ GeV is determined by hadronic collisions with center-of-mass energies larger than the maximum LHC energy. Similarly, the results presented in the right panel indicate that, for $E_\nu \gtrsim 10^5$ GeV, the neutrino flux receives a large contribution from collisions where x_2 is smaller than 10^{-5}, independent of the primary flux model used in the calculations. These results indicate that the main conclusions derived in this paper for the kinematical regions that determine the neutrino flux are almost insensitive to the model used to describe the primary nucleon flux.

The sensitivity of our predictions on the PDF choice is presented in Fig. 8, where we show the distributions in Feynman x_F for two different parton distribution sets and for two different energies of the incident cosmic rays, assumed to be protons. In particular, we will compare our previous estimates obtained using the CT14LL parametrization [29], with those derived using the MMHT2014LO one [38]. For completeness, in Fig. 8 we also show the contribution of the quark-antiquark annihilation process. Here, both PDF sets give quite similar cross sections for both energies. Regarding the $gg \to c\bar{c}$ contribution, one finds that at lower energies (left panel) both PDF sets give the same x_F distributions, while at higher energies (right panel) they lead to quite different results. Clearly, the present experimental data obtained at the LHC cannot constrain the gluon distributions at $x < 10^{-5}$. Since variations in the x_F distribution at intermediate values of x_F have a direct impact on the neutrino flux, we are forced to conclude that the current predictions for the prompt neutrino flux at very high neutrino energies are still not reliable.

The description of the QCD dynamics at small-x and the heavy quark production at large energies and forward rapidities are currently the subjects of intense debate. Basically, different formalisms based on different assumptions are able to describe the current experimental data. As the behavior of the prompt neutrino flux at high energies is determined by the x_F distribution at intermediate values of x_F, it is interesting to compare the predictions of these formalisms for energies probed in neutrino physics. In Fig. 9, we compare the charm production cross section obtained in different underlying QCD approaches: the collinear factorization approach (solid and dotted lines), the k_T factorization approach [39–42] (dashed line), and the dipole model accounting for the saturation phenomena [43–45] (dashed-dotted line). These distinct approaches for the heavy quark production in hadronic collisions differ in their basic assumptions and partonic pictures.

While in the collinear framework, all particles involved are assumed to be on mass shell, carrying only longitudinal momenta, and the cross section is averaged over two transverse polarizations of the incident gluons, in the k_T factorization approach, the Feynman diagrams are calculated taking into account the virtualities and all possible polarizations of the incident partons. Moreover, in the k_T factorization approach, the unintegrated gluon distributions are employed instead of the usual collinear distributions.

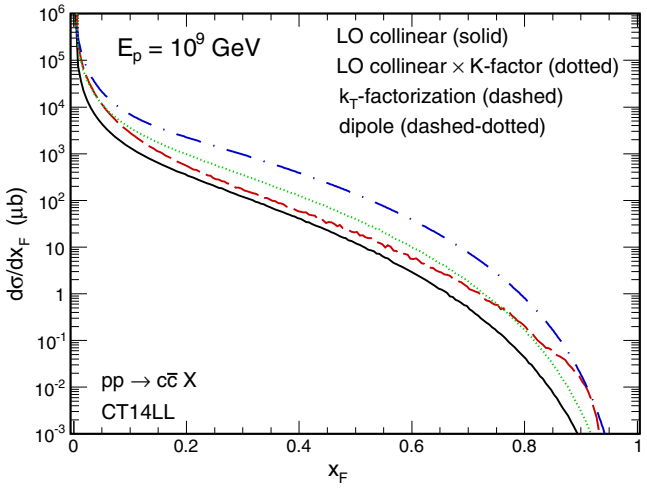

FIG. 9. Charm production cross section $d\sigma/dx_F$ obtained with three difference QCD approaches: collinear factorization (solid and dotted lines), k_T factorization with the KMR UGDF (dashed line), and dipole model presented in Refs. [46,47] (dashed-dotted line).

In contrast, in the color dipole formalism [43–45], the basic partonic picture of heavy quark production in gluon-gluon interactions is such that, before interacting with the hadron target, a gluon is emitted by a projectile and fluctuates into a color octet pair $Q\bar{Q}$, its lowest-order Fock component. The dipole approach does not rely on QCD factorization [48] and is based upon the universal ingredients, such as the dipole cross section and the light-cone wave function, for a given Fock component of the projectile that undergoes scattering off the target nucleon. One of the main motivations to use this approach is that it allows us to take into account the nonlinear effects in the QCD dynamics, expected to be important at large energies, and the QCD factorization breaking effects at large Feynman x_F, as well as the higher-order QCD corrections and coherence phenomena (for more details, see, e.g., Refs. [46,49–52] and references therein).

The framework of k_T factorization used here was successfully applied by two of us for single [53] and double [54] open charm meson production at the LHC, as well as for leptons from semileptonic decays of heavy mesons at the relativistic heavy ion collider (RHIC) [55]. As a default choice, we use the Kimber-Martin-Ryskin (KMR) [56,57] unintegrated gluon distribution functions (UGDFs), which were shown recently to effectively include a part of real higher-order corrections in charm production [58]. In the case of the dipole approach, we will consider the predictions obtained recently in Refs. [46,47], which describe the current LHCb data, at least in the high-p_T domain. As discussed above, here the Feynman x_F distributions are very sensitive to the very small transverse momenta.

We observe in Fig. 9 a significant order-of-magnitude difference between the predictions of the dipole and collinear QCD approaches, with the k_T factorization result being in between. We wish to point out here that the contributions of the gluon bremsstrahlung off light $q \to q + (G \to Q\bar{Q})$ and heavy $Q(\bar{Q}) \to Q(\bar{Q}) + G$ (anti) quarks are not included in the current dipole-model analysis and are worth further exploration. The large cross section in the dipole model is somewhat unexpected, as this approach includes saturation effects that should lead rather to a reduction of the cross section compared with the traditional collinear factorization approach. On the other hand, a similar effect has been observed at low heavy quark (heavy meson) transverse momenta $p_T < m_Q$ where the dipole results overshoot the LHC data on open heavy flavor production [46]. Can this effect be caused by an approximate treatment of the kinematics and the dipole cross section or due to the missing higher-Fock (higher-twist) contributions in the current dipole-model analysis? Recently, the Drell-Yan process in the dipole picture and the associated kinematic constraints were thoroughly discussed by some of us in Refs. [51,52,59], while the higher-twist corrections remain uncertain. A proper analysis of this issue for heavy flavor production in the dipole picture is left for a future work.

In the perturbative (high-p_T, $p_T > m_Q$) domain, the k_T factorization with the KMR unintegrated gluon distribution and next-to-leading collinear factorization give very similar results, which does not need to be so with different unintegrated gluon distributions. The dipole approach should work intentionally at a small-x region, but usually works also at intermediate x range. So in the intermediate x range, the dipole and k_T factorization approaches are known to give similar results as the next-to-leading order collinear factorization approach. At very low-x region, the dipole approach, which includes saturation effects, may produce different results than the collinear and k_T factorization approaches.

The low-p_T results of the k_T factorization approach are rather uncertain due to uncertainties in the unintegrated gluon PDFs in the nonperturbative region of small gluon transverse momenta. Also, both very low-x ($x < 10^{-5}$) and low-p_T ($p_T < m_Q$) regions are not very trustworthy due to the absence of the potentially relevant saturation effects that become important in these kinematic domains. Finally, the k_T factorization may be broken at very large x_F. The results of the k_T factorization and leading-order collinear factorization approaches may substantially differ in these kinematic domains.

Although the dipole approach does not rely on factorization in the target nucleon, it incorporates the saturation physics. There is still a problem of its prediction relying on factorization over the projectile nucleon, especially for heavy quark studies. Assuming the $gg \to Q\bar{Q}$ process is the dominant mechanism at large x_F, there is a problem of the projectile gluon PDF at large x entering this process. Besides, at low quark p_T's, the primordial k_T distribution

of the projectile gluon becomes important, but it is largely unknown (the existing models predict a very big uncertainty there). Finally, a potentially large fraction of intrinsic heavy flavor in the projectile nucleon is not included here and deserves a dedicated work.

Before drawing any strong conclusions on the prompt neutrino flux, one would need to improve our theoretical understanding, at least of the primordial gluon p_T distribution, as well as on the relevance of saturation and factorization-breaking effects at large x_F.

Finally, in Fig. 10, we show the six-year experimental data collected by the IceCube Observatory [3] together with our predictions for the neutrino flux, calculated with two different current gluon PDFs. Both theoretical fluxes are below the IceCube data, but unfortunately, at present, we cannot draw too strong conclusions. For comparison, we show the result of a simple fit (unbroken power-law isotropic distribution) proposed in Ref. [3], which is consistent with the as-yet low-statistics data.

Considering the several aspects discussed above, one finds that, in order to disentangle the magnitude of the astrophysical contribution to the neutrino flux, it is mandatory to get a better theoretical control of the prompt neutrino flux. Although the new experimental data from the LHC will be useful, they will not well constrain the charm production and QCD dynamics in the kinematical ranges that determine the prompt neutrino flux at IceCube and future neutrino telescopes. Therefore, the experimental measurement of the neutrino flux and the separation of the prompt contribution are important challenges that should be surpassed in order to improve our understanding of strong interactions at high energies as well as of neutrino physics in astrophysical events.

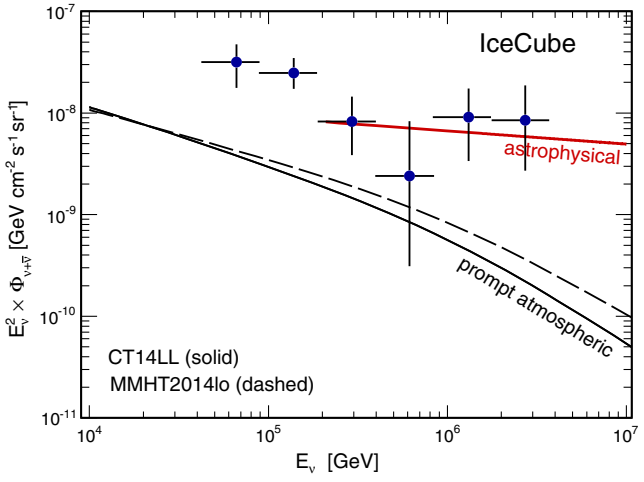

FIG. 10. Comparison of predictions obtained with the CT14 and MMHT PDFs for the prompt neutrino flux. The data points are taken from Ref. [3]. For comparison, the fit for the astrophysical contribution, proposed in Ref. [3], is presented as well.

IV. SUMMARY

One of the current challenges in neutrino physics is to disentangle the signals of astrophysical origin from those associated with atmospheric interactions. The precise determination of the conventional and prompt atmospheric neutrino fluxes is fundamental for the interpretation of the results from neutrino observatories, such as IceCube. In the last years, several groups estimated the prompt neutrino flux using different theoretical approaches, e.g., for the calculation of the charm production cross section, charm fragmentation, cosmic ray flux, etc. These studies demonstrated that the theoretical uncertainties are large, although they were reduced by the recent collider data and theoretical developments for the heavy quark production. Consequently, it is important to map the kinematical range that is probed by high-energy atmospheric neutrinos in order to clearly define the next steps that should be performed to obtain precise predictions for the atmospheric neutrino flux. This has been one of the main goals of our current study.

In this paper, we have presented a detailed analysis of the kinematical domains that dominate the charm and prompt atmospheric neutrino production in cosmic rays relevant for the IceCube experiment by exploring the sensitivity of the corresponding neutrino flux and the charm cross section to the cuts on the maximal pp c.m. energy, the longitudinal momentum fraction in the target and projectile, and the Feynman x_F and p_T variables included in the calculation. We have found that, in order to address production of high-energy neutrinos ($E_\nu > 10^7$ GeV), one needs to know the charm production cross section for energies larger than those available at the LHC, as well as the parton/gluon distributions for the longitudinal momentum fractions in the region $10^{-8} < x < 10^{-5}$. Since this region of x is not available at the collider measurements at the moment, the predictions in the collinear factorization approach and the k_T factorization approach are not very reliable. If it was possible to disentangle the prompt atmospheric contribution from the cosmogenic one, it could perhaps become possible to put some constraints on the gluon distributions for extremely small longitudinal momentum fractions. This option requires a more dedicated study in the future.

We have also indicated the characteristic theoretical uncertainties in the charm production cross section obtained within different QCD approaches typically used by different groups in the analysis of prompt neutrino fluxes, such as the leading-order collinear factorization approach, k_T factorization, and the dipole model accounting for the saturation phenomena.

Our results demonstrate that, in order to predict the prompt neutrino flux for typical neutrino energies at the IceCube Observatory and future neutrino telescopes, we should extrapolate the behavior of the heavy quark cross sections and energy distributions beyond the range accessible experimentally by current collider measurements.

These results indicate that theoretical and experimental studies of the prompt atmospheric neutrino flux can provide important information about the mechanism of heavy quark production, as well as the description of the QCD dynamics in a kinematical range beyond that reached by the current colliders. At the current stage of research, it is premature to decide whether the measurement at the IceCube Observatory can provide new information on the gluon distribution at very low longitudinal fractions $x \sim 10^{-7}$.

ACKNOWLEDGMENTS

V. P. G. is partially supported by CNPq, Brazil. R. P. is partially supported by the Swedish Research Council, Contract No. 621-2013-428 and by CONICYT Grant No. PIA ACT1406. R. M. and A. S. were partially supported by the Polish National Science Center Grant No. DEC-2014/15/B/ST2/02528. A. S. thanks Tomasz Palczewski for explaining some details about the IceCube Observatory and related physics.

[1] M. G. Aartsen *et al.* (IceCube Collaboration), Science **342**, 1242856 (2013).
[2] M. G. Aartsen *et al.* (IceCube Collaboration), Phys. Rev. Lett. **113**, 101101 (2014).
[3] M. G. Aartsen *et al.* (IceCube Collaboration), Astrophys. J. **833**, 3 (2016).
[4] F. Halzen and S. R. Klein, Rev. Sci. Instrum. **81**, 081101 (2010).
[5] R. Abbasi *et al.* (IceCube Collaboration), Phys. Rev. D **83**, 012001 (2011).
[6] M. G. Aartsen *et al.* (IceCube Collaboration), Phys. Rev. Lett. **110**, 151105 (2013).
[7] P. Adamson *et al.* (MINOS Collaboration), Phys. Rev. D **86**, 052007 (2012).
[8] Y. Fukuda *et al.* (Super-Kamiokande Collaboration), Phys. Lett. B **436**, 33 (1998).
[9] M. Honda, T. Kajita, K. Kasahara, S. Midorikawa, and T. Sanuki, Phys. Rev. D **75**, 043006 (2007).
[10] G. D. Barr, T. K. Gaisser, P. Lipari, S. Robbins, and T. Stanev, Phys. Rev. D **70**, 023006 (2004).
[11] T. K. Gaisser and S. R. Klein, Astropart. Phys. **64**, 13 (2015).
[12] P. Gondolo, G. Ingelman, and M. Thunman, Astropart. Phys. **5**, 309 (1996).
[13] A. D. Martin, M. G. Ryskin, and A. M. Stasto, Acta Phys. Pol. B **34**, 3273 (2003).
[14] M. V. Garzelli, S. Moch, and G. Sigl, J. High Energy Phys. 10 (2015) 115.
[15] A. Bhattacharya, R. Enberg, M. H. Reno, I. Sarcevic, and A. Stasto, J. High Energy Phys. 06 (2015) 110.
[16] R. Gauld, J. Rojo, L. Rottoli, and J. Talbert, J. High Energy Phys. 11 (2015) 009.
[17] A. Bhattacharya, R. Enberg, Y. S. Jeong, C. S. Kim, M. H. Reno, I. Sarcevic, and A. Stasto, J. High Energy Phys. 11 (2016) 167.
[18] R. Gauld, J. Rojo, L. Rottoli, S. Sarkar, and J. Talbert, J. High Energy Phys. 02 (**2016**) 130.
[19] F. Halzen and L. Wille, Phys. Rev. D **94**, 014014 (2016).
[20] R. Laha and S. J. Brodsky, arXiv:1607.08240.
[21] M. V. Garzelli, S. Moch, O. Zenaiev, A. Cooper-Sarkar, A. Geiser, K. Lipka, R. Placakyte, and G. Sigl (PROSA Collaboration), J. High Energy Phys. 05 (2017) 004.
[22] M. Benzke, M. V. Garzelli, B. Kniehl, G. Kramer, S. Moch, and G. Sigl, arXiv:1705.10386.
[23] R. Aaij *et al.* (LHCb Collaboration), Nucl. Phys. **B871**, 1 (2013).
[24] R. Aaij *et al.* (LHCb Collaboration), J. High Energy Phys. 03 (2016) 159; 09 (2016) 13; 05 (2017) 74.
[25] R. Enberg, M. H. Reno, and I. Sarcevic, Phys. Rev. D **78**, 043005 (2008).
[26] L. Pasquali, M. H. Reno, and I. Sarcevic, Phys. Rev. D **59**, 034020 (1999).
[27] M. G. Aartsen *et al.* (IceCube Collaboration), arXiv: 1412.5106.
[28] B. L. Combridge, Nucl. Phys. **B151**, 429 (1979).
[29] J. Gao, M. Guzzi, J. Huston, H.-L. Lai, Z. Li, P. Nadolsky, J. Pumplin, D. Stump, and C.-P. Yuan, Phys. Rev. D **89**, 033009 (2014).
[30] A. Cisek, W. Schäfer, and A. Szczurek, J. High Energy Phys. 04 (2015) 159.
[31] A. Szczurek, A. Cisek, and W. Schafer, Acta Phys. Pol. B **48**, 1207 (2017).
[32] V. P. Goncalves, L. A. S. Martins, and W. K. Sauter, Eur. Phys. J. C **76**, 97 (2016); V. P. Goncalves, B. D. Moreira, and F. S. Navarra, Phys. Rev. D **95**, 054011 (2017).
[33] R. D. Ball *et al.* (NNPDF Collaboration), J. High Energy Phys. 04 (2015) 040.
[34] R. Gauld and J. Rojo, Phys. Rev. Lett. **118**, 072001 (2017).
[35] E. G. de Oliveira, A. D. Martin, and M. G. Ryskin, arXiv: 1705.08845.
[36] R. Gauld, J. Rojo, and E. Slade, arXiv:1705.04217.
[37] S. Ter-Antonyan, Phys. Rev. D **89**, 123003 (2014).
[38] L. A. Harland-Lang, A. D. Martin, P. Motylinski, and R. S. Thorne, Eur. Phys. J. C **75**, 204 (2015).
[39] L. V. Gribov, E. M. Levin, and M. G. Ryskin, Phys. Rep. **100**, 1 (1983).
[40] S. Catani, M. Ciafaloni, and F. Hautmann, Phys. Lett. B **242**, 97 (1990).
[41] S. Catani, M. Ciafaloni, and F. Hautmann, Nucl. Phys. **B366**, 135 (1991).
[42] J. C. Collins and R. K. Ellis, Nucl. Phys. **B360**, 3 (1991).
[43] B. Z. Kopeliovich, L. I. Lapidus, and A. B. Zamolodchikov, JETP Lett. **33**, 595 (1981).

[44] N. N. Nikolaev, G. Piller, and B. G. Zakharov, Zh. Eksp. Teor. Fiz. **108**, 1554 (1995) [J. Exp. Theor. Phys. **81**, 851 (1995)]; Z. Phys. A **354**, 99 (1996).
[45] B. Z. Kopeliovich and A. V. Tarasov, Nucl. Phys. **A710**, 180 (2002).
[46] V. P. Goncalves, B. Kopeliovich, J. Nemchik, R. Pasechnik, and I. Potashnikova, Phys. Rev. D **96**, 014010 (2017).
[47] F. Carvalho, A. V. Giannini, V. P. Goncalves, and F. S. Navarra, Phys. Rev. D **96**, 094002 (2017).
[48] B. Z. Kopeliovich, J. Nemchik, I. K. Potashnikova, M. B. Johnson, and I. Schmidt, Phys. Rev. C **72**, 054606 (2005).
[49] J. Raufeisen and J. C. Peng, Phys. Rev. D **67**, 054008 (2003).
[50] R. Pasechnik, B. Kopeliovich, and I. Potashnikova, Adv. High Energy Phys. **2015**, 701467 (2015).
[51] E. Basso, V. P. Goncalves, J. Nemchik, R. Pasechnik, and M. Sumbera, Phys. Rev. D **93**, 034023 (2016).
[52] V. P. Goncalves, M. Krelina, J. Nemchik, and R. Pasechnik, Phys. Rev. D **94**, 114009 (2016).
[53] R. Maciuła and A. Szczurek, Phys. Rev. D **87**, 094022 (2013).
[54] R. Maciuła and A. Szczurek, Phys. Rev. D **87**, 074039 (2013).
[55] R. Maciuła, A. Szczurek, and M. Łuszczak, Phys. Rev. D **92**, 054006 (2015).
[56] M. A. Kimber, A. D. Martin, and M. G. Ryskin, Phys. Rev. D **63**, 114027 (2001).
[57] G. Watt, A. D. Martin, and M. G. Ryskin, Phys. Rev. D **70**, 014012 (2004); **70**, 079902(E) (2004).
[58] R. Maciuła and A. Szczurek, Phys. Rev. D **94**, 114037 (2016).
[59] W. Schäfer and A. Szczurek, Phys. Rev. D **93**, 074014 (2016).